Taste buds are not derived from neural crest in mouse, chicken, and zebrafish

Wenxin Yu, Zhonghou Wang, Brett Marshall, Yuta Yoshida, Renita Patel, Xiaogang Cui, Rebecca Ball, Linlin Yin, Fuminori Kawabata, Shoji Tabata, Wenbiao Chen, Robert N. Kelsh, James D. Lauderdale, Hong-Xiang Liu

PII: S0012-1606(20)30321-3

DOI: https://doi.org/10.1016/j.ydbio.2020.12.013

Reference: YDBIO 8360

To appear in: *Developmental Biology*

Received Date: 9 October 2020

Revised Date: 10 December 2020

Accepted Date: 11 December 2020

Please cite this article as: Yu, W., Wang, Z., Marshall, B., Yoshida, Y., Patel, R., Cui, X., Ball, R., Yin, L., Kawabata, F., Tabata, S., Chen, W., Kelsh, R.N., Lauderdale, J.D., Liu, H.-X., Taste buds are not derived from neural crest in mouse, chicken, and zebrafish, *Developmental Biology* (2021), doi: https://doi.org/10.1016/j.ydbio.2020.12.013.

Taste buds are not derived from neural crest in mouse, chicken, and zebrafish

Wenxin Yu[1,2 &], Zhonghou Wang[1,2 &], Brett Marshall[1,2 &], Yuta Yoshida[1,2 #], Renita Patel[1,2], Xiaogang Cui[1,2 #], Rebecca Ball[3], Linlin Yin[4], Fuminori Kawabata[5 #], Shoji Tabata[5], Wenbiao Chen[4], Robert N. Kelsh[6], James D. Lauderdale[1,3], Hong-Xiang Liu[1,2 *]

[1]Regenerative Bioscience Center; [2]Department of Animal and Dairy Science, College of Agricultural and Environmental Sciences; [3]Department of Cellular Biology, Franklin College of Arts and Sciences; The University of Georgia, Athens, GA, USA.

[4]Department of Molecular Physiology and Biophysics, School of Medicine, Vanderbilt University, Nashville, TN, USA.

[5]Laboratory of Functional Anatomy, Faculty of Agriculture, Kyushu University, Fukuoka, Japan.

[6]Department of Biology and Biochemistry, University of Bath, Claverton Down, Bath, UK.

[&] These authors contributed equally to the work.

[#]Present address: (YY) Department of Food and Life Sciences, College of Agriculture, Ibaraki University, Ami, Japan; (XC) Institutes of Biomedical Sciences, Key Laboratory of Chemical Biology and Molecular Engineering of National Ministry of Education, Shanxi University, Taiyuan, China; and (FK) Physiology of Domestic Animals, Faculty of Agriculture and Life Science, Hirosaki University, Hirosaki, Japan.

*Correspondence to: Hong-Xiang Liu, Regenerative Bioscience Center, Department of Animal and Dairy Science, College of Agricultural and Environmental Sciences, University of Georgia, 425 River Road, Athens, GA 30602, USA. Email: lhx@uga.edu

Running title: Neural crest cells are not progenitors for taste buds

Abstract

Our lineage tracing studies using multiple *Cre* mouse lines showed a concurrent labeling of abundant taste bud cells and the underlying connective tissue with a neural crest (NC) origin, warranting a further examination on the issue of whether there is an NC derivation of taste bud cells. In this study, we mapped NC cell lineages in three different models, *Sox10-iCreER^{T2}/tdT* mouse, GFP^{+} neural fold transplantation to GFP^{-} chickens, and *Sox10-Cre/GFP-RFP* zebrafish model. We found that in mice, *Sox10-iCreER^{T2}* specifically labels NC cell lineages with a single dose of tamoxifen at E7.5 and that the labeled cells were widely distributed in the connective tissue of the tongue. No labeled cells were found in taste buds or the surrounding epithelium in the postnatal mice. In the GFP^{+}/GFP^{-} chicken chimera model, GFP^{+} cells migrated extensively to the cranial region of chicken embryos ipsilateral to the surgery side but were absent in taste buds in the base of oral cavity and palate. In zebrafish, *Sox10-Cre/GFP-RFP* faithfully labeled known NC-derived tissues but did not label taste buds in lower jaw or the barbel. Our data, together with previous findings in axolotl, indicate that taste buds are not derived from NC cells in rodents, birds, amphibians or teleost fish.

Keywords: Taste buds, neural crest, progenitors, mouse, chicken, zebrafish.

Introduction

Taste buds are taste sensory organs located on the tongue and inside the oral cavity of all vertebrates. In some fishes and amphibians, particularly species with barbels, taste buds are also found in the skin. A large proportion of taste bud cells are glial-like (type I) (1-6) and a small subset is neuronal-like (type III) (3, 7-11). Given that glial cells in the peripheral nervous system are derived from the neural crest (NC) (12-15) and neurons are from either NC (13-18) or epibranchial placodes (15, 19-24), a question has been asked whether taste buds could plausibly have been derived either from the NC, or from the epibranchial placodes, or from the local epithelium (25). Barlow and Northcutt used grafting experiments between pigmented and non-pigmented axolotl embryos and showed that neither the NC nor epibranchial placodes contribute to taste buds, whereas DiI-labeled endoderm formed both taste buds and the surrounding epithelium in the oropharynx, confirming an endoderm-derived local epithelial origin for taste buds in axolotl (25).

Although compelling evidence demonstrates a non-NC origin of taste bud cells in axolotl (25), studies in rodents indicate that, in addition to the lingual epithelium (26-31), NC may also contribute to taste bud cells (32-34). This difference between axolotl and rodents suggests that there may be a difference in taste bud development between non-mammals and mammals.

In mice, evidence that taste bud progenitors arise from local epithelium is solid (25-31). Stone and colleagues identified local epithelium as taste progenitor source using mosaic X-inactivation chimera mouse model (28), which was later reiterated by Okubo and colleagues who traced the lineage of local epithelium to taste buds using *Cre-LoxP* transgenic mouse

model (29). However, the question remains whether surrounding epithelium is the “sole” source of taste bud progenitors.

In the past several years, the use of transgenic mouse lines to trace the lineage of cranial NC cells has raised new speculations regarding NC derivatives, e.g., tooth bud (35) and olfactory (36, 37) epithelial cells. In the tongue organ, NC has been found to be the major contributor to the mesenchyme (38) and connective tissue under the epithelium (32-34). Our recent findings revealed that a significant proportion of taste bud cells are labeled with *P0-Cre* (33, 34), *Dermo1-Cre* (33), *Sox10-Cre* (32) concurrently with the underlying connective tissue cells in the absence of labeling in the surrounding lingual epithelium. In contrast, *Wnt1-Cre*-labeled cells are rarely seen in taste buds although labeled cells are extensive in the underlying connective tissue (34). Therefore, the published data suggest the possibility of a NC derivation of taste buds (32-34) but this fundamental issue has not yet settled. Given that none of these models labels all NC cells, nor do they label NC cells exclusively (39, 40), animal models that specifically and exclusively label NC cell lineages and detailed examinations are imperative.

To address the fundamental issues of whether taste bud cells have a derivation from NC cells and whether this contribution is species-specific, we performed lineage tracing for NC cells in three model species, using *Sox10-iCreER^{T2}/tdT* mice, GFP^{+}/GFP^{-} chicken chimeras, and *Sox10-Cre/GFP-RFP* zebrafish. We found that in these three models NC cell lineages were extensively marked but not found in taste buds. Together with previous findings in axolotl (25), the data from these different model species provide support for the idea that taste buds do not have a NC derivation.

Materials and Methods

Animals

Animal use was approved by The University of Georgia Institutional Animal Care and Use Committee and was in accordance with the National Institutes of Health Guidelines for care and use of animals for research. Three species of animals were used: mouse, chicken and zebrafish.

Mice were maintained and bred in the animal facility of the Animal and Dairy Science department at the University of Georgia at 22℃ under 12-hr day/night cycles. *Sox10-iCreER^{T2}* (CBA;B6-Tg(Sox10-icre/ER^{T2})388Wdr/J, Stock#027651) (41) and *R26-tdTomato* (hereafter tdT) *Cre* reporter mice (B6.Cg-*Gt(ROSA)26Sor$^{tm14(CAG-tdTomato)Hze}$*/J, Stock#007914) (42) were obtained from The Jackson Laboratory. The hemizygous *Sox10-iCreER^{T2}* mice and homozygous *tdT* reporter breeders were crossed to generate *Sox10-iCreER^{T2}/tdT* mice. No significant difference was found in the distribution pattern of labeled cells between males and females; therefore, males and females were grouped together and used at the examined stages. *Cre* negative littermates served as controls. FVB/J wild type mice (129;FVB-Tmem79^{m1J}/GrsrJ, The Jackson Laboratory, Stock#014103) were used to breed in parallel for fostering caesarean born *Sox10-iCreER^{T2}/tdT* pups.

Chicken embryos were produced by incubating fertilized eggs horizontally in the cabinet incubator (Cat#1502 “SPORTSMAN”, GQF Manufacturing Company, Inc, Savannah, GA) in the lab room at the University of Georgia. Fertilized Roslin GFP^{+} donor (43) and Roslin GFP^{-} host chicken eggs were purchased from Clemson University.

Zebrafish were housed in the Paul D. Coverdell Building Fish Facility at the University of

Georgia at 28.5℃ under 12-hr day/night cycles. *Sox10-EGFP* zebrafish (TG(*-4.9sox10:egfp*)^{ba2} and *Sox10-Cre* zebrafish (*TG*(*-4725sox10:Cre)*^{ba74} were obtained from Dr. Robert N. Kelsh, University of Bath, Bath, UK) (44-46). Hemizygous *Sox10-Cre* zebrafish (*TG*(*-4725sox10:Cre)*^{ba74} were crossed with homozygous *GFP-RFP Cre* reporter zebrafish (*Tg(eab2:[EGFP-T-mCherry])*, from Dr. Wenbiao Chen, Vanderbilt University, Nashville, TN) (47) to generate *Sox10-Cre/GFP-RFP* zebrafish. Timed pairings were allowed for 30 min for synchronized embryo development.

PCR genotyping was performed using the following primers: (1) mouse *Cre* allele forward 5'-ATT GCT GTC ACT TGG TCG GC-3' and reverse 5'-GGA AAA TGC TTC TGT CCG TTT GC-3' to detect the mouse *Cre* recombinase allele; (2) zebrafish *Cre* allele forward 5'-CCA TGT CCA AAT TTA CTG ACC GTA C-3' and reverse 5'-CAT CTT CAG GTT CTG CGG GAA AC-3' to detect the zebrafish *Cre* recombinase allele; (3) zebrafish *EGFP* allele forward 5'-GTT CAT CTG CAC CAC CGG C-3' and reverse 5'-TTG TGC CCC AGG ATG TTG C -3' to detect the zebrafish *EGFP* reporter allele; (4) *iCreER*^{T2} allele forward 5'-GAG ACG GAC CAA AGC CAC T-3' and reverse 5'-CTG CAG CCT CCT CCA CTG-3' to detect the mouse *iCreER*^{T2} recombinase allele; and (5) msSRYz_SexDet forward, 5'-TTG TCT AGA GAG CAT GGA GGG CCA TGT CAA-3' and reverse 5'-CCA CTC CTC TGT GAC ACT TTA GCC CTC CGA-3' to determine the sex of mouse embryos. *tdT* allele forward, 5'-CTG TTC CTG TAC GGC ATG G-3' and reverse 5'-GGC ATT AAA GCA GCG TAT CC-3' to determine the expression of *tdT* reporter.

Tamoxifen treatment of mice and pups fostering

Timed pregnant mice were used for labeling NC cell lineages specifically. Noon of the day

of vaginal plug detection in mice was designated embryonic (E) day 0.5. To induce *Cre* recombination in embryos at E8.0, tamoxifen (Tmx) (Cat No. T5648; Sigma-Aldrich, St. Louis, MO) was dissolved in corn oil at a concentration of 11.1 mg/mL, and a single dose of 0.1 mL tamoxifen solution was given through oral gavage using 16 G x 38 mm polyurethane feeding tubes (Cat No. FTPU-16-50, Instech Laboratories, Inc, Plymouth Meeting, PA) to the pregnant dams carrying E7.5 embryos ($Tmx^{@E7.5}$). Vehicle (Veh) controls were treated with corn oil at the same stage.

Tamoxifen injection in pregnant mice has been reported to cause dystocia. To resolve this problem, caesarean sections were performed to deliver the *Sox10-iCreER^{T2}/tdT* embryos at E18.5. The delivered pups were fostered by a FVB/J nursing dam immediately after caesarean birth.

GFP^+ neural fold transplantation in GFP^- chicken embryos

At Hamburger Hamilton 9 stage (29-33 hr post-incubation), a window on the eggshell was opened above the embryos. A drop of sterile 0.5% neutral red (Cat No. N2889-100ML, Sigma-Aldrich, St. Louis, MO) in 0.9% NaCl was used to stain and stage the embryos under a dissection microscope. According to the previous report that an “insertion” instead of “replacement” of neural folds for graft transplantation increased the survival rate while maintaining the normal development of NC and NC-derived organs (48), a single side of neural fold at the levels of posterior midbrain and anterior hindbrain were dissected from a GFP^+ chicken embryo and inserted into the lesion made laterally adjacent to the counterpart of a GFP^- chicken embryo at the same somite stage. After the surgery, embryos were incubated until desired stages ranging from 1-19 days post-surgery (DPS).

Tissue collections

Mouse embryos at embryonic E8.0-8.5 were collected between 10am and 4pm. The embryos were also staged by counting somite pairs. Embryos at 7~15-somite stages (n=4 for both vehicle- and tamoxifen-treated groups) were selected and used for further analyses. Pregnant dams were euthanized with CO_2 followed by cervical dislocation. The uterus was removed and placed in a petri dish containing 0.1 M phosphate buffered saline (PBS) (Cat No. CP4390-48, Denville Scientific, Inc, Metuchen, NJ). Embryos were dissected from the uterus under a stereomicroscope and fixed with 4% paraformaldehyde (PFA) (Cat No. AAJ19943k2, Fisher HealthCare, Houston, TX) in 0.1 M PBS at 4℃ for 2 hr. Postnatal mice were harvested at 2 wk, 4 wk, and 8 wk (n=3 for both vehicle- and tamoxifen-treated at each stage). Mice were euthanized with CO_2 followed by transcardial perfusion using 10 mL warm 0.1 M PBS, followed by 10 mL warm and 20 mL cold 2% PFA in 0.1 M PBS. Tongues, soft palates, heads, and dorsal root ganglia were dissected and further fixed in 2% PFA at 4℃ for 2 hr.

GFP^+/GFP^- chicken chimeras with successful transplantation were collected at 1 (n=5), 2 (n=2), 14 (n=2), and 19 (n=5) DPS. Palates and base of oral cavities were dissected from embryos at 14 and 19 DPS. Whole embryos at 1 and 2 DPS and dissected tissues at 14 and 19 DPS were then fixed with 4% PFA in 0.1 M PBS at 4℃ for 2 hr.

Zebrafish eggs were collected after 1 hr pairing and incubated in 28.8℃ egg water until collections at 7- (n=3), 10- (n=3), and 12-somite (n=3) stages and 5.5 (n=3), 15 (n=3), and 30 (n=3) days post fertilization (dpf) and adult (90 days to 2 years) (n=3). Zebrafish were anesthetized with a neutrally-buffered solution of 0.016% Tricaine (Cat No. T0941, TCI AMERICA, Portland, OR), followed by decapitation and fixation in 4% PFA at 4℃ for 2 hr. For

30-day-old and adult fish, fixed heads were further treated with 0.5 M EDTA (Cat No. RES3002E, Sigma-Aldrich, St. Louis, MO) for bone softening, with medium change every other day for 2 wk.

Immunohistochemistry

All fixed tissues were cryoprotected in 30% sucrose in 0.1 M PBS for at least 48 hr at 4℃. Tissues were trimmed and dissected, embedded in O.C.T. (Cat No. 23-730-571, Fisher Healthcare, Houston, TX) and rapidly frozen as such for: (1) Mice: transverse sections of cranial region of E8.5 embryos, sagittal sections of whole tongue of E12.5 embryos, sagittal sections of the left and right halves of the anterior 2/3 of postnatal oral tongue where fungiform papillae are distributed, sagittal sections of both foliate papillae, left and right halves of soft palate, and coronal sections of single circumvallate papilla; (2) Chickens: transverse sections of cranial region of embryos at 1 DPS, sagittal sections of whole embryos at 2 DPS, base of oral cavities of embryos at 14 and 19 DPS, and palates of embryos at 19 DPS; (3) Zebrafish: horizontal sections of zebrafish embryos, sagittal sections of heads of 5.5- and 15-dpf-old fish, sagittal sections of lower jaws, barbels, and body segments of 30-dpf and adult fish.

Frozen sections were cut at 8 μm in thickness and mounted onto charged slides (Fisher brand™ Superfrost™ Plus Microscope Slides, Cat No. 12-550-15, Fisher Scientific, Waltham, MA). Non-specific binding was blocked with 10% normal donkey serum (Cat No. SLBW2097, Sigma-Aldrich, St. Louis, MO) in 0.1 M PBS containing 0.3% Triton X-100 (Cat No. X100-100ML, Sigma-Aldrich, St. Louis, MO) for 30 min, followed by overnight incubation with primary antibody diluted with 0.1 M PBS containing 0.3% Triton X-100 and 1% normal donkey

serum. Primary antibodies used in this study are listed in Table 1.

After rinses in 0.1 M PBS (3 times, 10 min each), sections were incubated in Alexa Fluor® 488 (for E-cadherin, GFP), Alexa Fluor® 546 (for dsRed), and/or Alexa Fluor® 647 (for all the other markers)-labeled secondary antibody (1:500, Invitrogen, Eugene, OR) for 1 hr at room temperature. Sections were rinsed and then counterstained with DAPI (200 ng/mL, Cat No. D1306, Fisher Scientific, Waltham, MA). After rinses with 0.1 M PBS followed by dipping in Milli-Q water (Direct-Q® 3 UV water purification system, Millipore, MA). Sections were air dried and coverslipped with Prolong® diamond antifade mounting medium (Cat No. P36970, Fisher Scientific, Waltham, MA).

Photomicroscopy

Immunoreacted sections on slides were analyzed under a fluorescent light microscope (EVOS FL, Life Technologies, CA) and images were taken using a laser scanning confocal microscope (Zeiss LSM 710, Zeiss, Germany). Whole mount tissues were examined and images taken using a stereomicroscope (Olympus, SZX116, Japan). Images were assembled using Adobe Photoshop with minimal editing.

Results

In mice, *Sox10-iCreER^{T2}* specifically and extensively labels NC cell lineages with a single dose of tamoxifen at E7.5 and labeled cells are not found in taste buds

In mouse embryos, *Sox10* expression has been found specifically in NC cells during early embryonic stages (49, 50). To exclusively map the lineages of *Sox10*$^{+}$ NC cells, we utilized a *Sox10-iCreER^{T2}* mouse model (41) in which *iCreER^{T2}* is driven by endogenous *Sox10* promoter and tamoxifen administration was performed at E7.5 when NC cells were about to

be generated (51, 52) and express *Sox10* (49, 50). To validate the specificity and recombination efficiency of *Sox10-iCreER*^{T2} in labeling NC cell lineages, *Sox10-iCreER*^{T2} expression were analyzed in vehicle and tamoxifen-treated mice (n=3 for each group). In transverse sections of E8.5 (12-somite) *Sox10-iCreER*^{T2} embryos at 1 day after a single-dose vehicle (corn oil) treatment to the pregnant dam at E7.5 (Veh$^{E7.5}$), Cre recombinases were detected exclusively in Sox10^{+} cranial NC cells (Figure 1A-B), including the cells in the trigeminal NC tissue (53) (Figure 1A), branchial arch 1 (Figure 1A), and optic eminence (Figure 1A). Importantly, Cre immunosignals were restricted to the cytoplasm (arrowheads) of the NC cells (Figure 1B). In the E8.5 (9-somite) *Sox10-iCreER*^{T2} embryos with tamoxifen treatment to the pregnant dam at E7.5 (Tmx$^{E7.5}$), Cre immunosignals were found within the nuclei (arrows) of Sox10^{+} NC cells (Figure 1C). In Tmx$^{E7.5}$ E12.5 *Sox10-iCreER*^{T2}*/tdT* embryos (n=3), tdT signals were obvious in the spatulate tongue (Figure 1D$_1$) and extensively distributed in the tongue mesenchyme under the epithelium (Figure 1D$_2$). In young adult (8 week, n=3) *Sox10-iCreER*^{T2} mice (Tmx$^{E7.5}$), tdT signals were found in tissue compartments that are known to arise from NC, including the dorsal root ganglia (Figure 1E). No tdT signals were found in corresponding *Cre*-negative control (data not shown). Together, a single dose of tamoxifen treatment to *Sox10-iCreER*^{T2} dam at E7.5 was sufficient to label NC cell lineages specifically and extensively.

To map the lineage of *Sox10*$^{+}$ NC-derived cells in taste buds, the distribution of *Sox10-iCreER*^{T2}*/tdT*-labeled cells (Tmx$^{E7.5}$) was thoroughly analyzed in the major tissues containing taste buds including the soft palate and all three types of lingual taste papillae, i.e., fungiform, foliate, and circumvallate, in 2-wk, 4-wk and 8-wk mice (n=3 for each stage). In

serial sections of the soft palate and tongue tissues, *Sox10-iCreER^{T2}* driven tdT^{+} cells were extensively distributed in the connective tissue (Figure 2A-C). In contrast, *Sox10-iCreER^{T2}/tdT*-labeled cells were not observed in taste buds located by the immunosignals of Krt8 in the soft palate (Figure 2C), and in all three types of lingual taste papillae, i.e., fungiform (Figure 2A-C), foliate (Figure 2C), circumvallate (Figure 2A-C). Additionally, tdT^{+} cells were not found in the taste bud-surrounding tongue epithelium, including basal epithelial cells that are known as progenitors of taste bud cells (26-31).

In GFP^{+}/GFP^{-} chicken chimera model, GFP^{+} NC cell lineages were labeled and sustained in the craniofacial regions, but not found in taste buds

To map GFP^{+} NC cell lineages in craniofacial regions, a GFP^{+}/GFP^{-} chimera chicken model was used. One side of neural folds at the posterior midbrain and anterior hindbrain levels was dissected from a transgenic GFP^{+} chicken (43) and then inserted into an incision lateral to the dorsal neural fold of a GFP^{-} chicken at the corresponding level of rostral-caudal axis (Figure 3A). At 1 day post-surgery (DPS) (n=5), ventrally migrating streams of GFP^{+} NC cells were observed in the transplantation side of the embryos (Figure 3B). To further validate the identity of GFP^{+} cells, HNK1 (54) was used to label migrating NC cells. GFP^{+} cells were largely, if not all, labeled by HNK1 (Figure 3C). Moreover, GFP^{+} NC cells were in the vicinity of ventral side of mesencephalon, which specifically contributes to oral tissues that host taste buds (Figure 3C).

To characterize the migration of NC lineages, chimeric embryos were collected at various stages. At 2 DPS (n=2), GFP^{+} cells populated at the ipsilateral side of pharyngeal arch to the neural fold insertion (Figure 4A), which would eventually give rise to oral tissues including

beaks. At 14 (n=2) and 19 DPS (n=5), GFP signals were detected in multiple craniofacial regions (Figure 4A). Of note, the GFP signals were remained restricted to the surgical side, which could be appreciated by a clear boundary in the midline separating GFP^+ and GFP^- tissues in the lower (Figure 4A) and upper (Figure 4A) beaks. Absence of GFP signals on the contralateral side of surgery was consistent in all examined chimeric embryos (Figure 4A).

In sagittal sections of surgical side of pharyngeal arch at 2 DPS and the bases of oral cavities at 14 and 19 DPS, GFP^+ cells were extensively and exclusively distributed in connective tissues immediately beneath the epithelium marked by EpCAM (Figure 4B). To further confirm whether there were GFP^+ cells in taste buds or not, thorough examinations were performed in serial sections of GFP^+ gustatory tissues in all surviving 19 DPS chimeric embryos (n=5) in which early taste buds have emerged. In the sections immunostained with a specific taste bud cell marker α-Gustducin, only the taste buds that were surrounded by GFP^+ connective tissue cells were included for analysis. A total of 40 taste buds from serial sections of GFP^+ base of oral cavities and 37 taste buds from serial sections of GFP^+ palates were imaged and analyzed. In contrast to the abundant distribution in the underlying connective tissue (Figure 5), GFP^+ cells were not observed in oral epithelium including taste buds and adjacent salivary glands in either the base of oral cavities (Figure 5A) or palates (Figure 5B).

In zebrafish, *Sox10*$^+$ NC cell lineage was not observed in taste buds

In addition to the use of mice and chickens, we introduced zebrafish, another widely used animal model for NC fate mapping (45, 55-60), to trace the lineage of *Sox10*$^+$ NC cells in taste buds. To verify the *Sox10* expression in NC cells and not in taste buds, *Sox10-EGFP* zebrafish (45, 46) were used (n=3 for each embryonic stage). In early embryos, EGFP

signals emerged in the trunk region at 7-somite stage (Figure 6A) and later appeared in cranial regions in 10- and 12-somite embryos (Figure 6A). Importantly, those signals were exclusively found in $Sox10^{+}$ NC cells (Figure 6B) in transverse sections of cranial region of 12-somite fish. Of note, in fish at 5.5 dpf (n=3), EGFP signals were absent in the taste buds marked by calretinin (Figure 6C).

The specific expression of *Sox10* in NC while being absent in fish taste buds allowed the use of *Sox10-Cre* fish model (44) to perform lineage tracing of $Sox10^{+}$ NC to taste buds. The use of *GFP-RFP* (47), in which the ubiquitous and constitutive *GFP* expression could be effectively switched to *RFP* upon *Cre* induced recombination, gave us a sharp contrast of signals for an easy recognition of *Cre*-labeled cells. *Sox10-Cre* driven RFP signals could be found in well-known NC-derived organs such as gills (Figure 6D) (61, 62). In lower jaw where most taste buds reside in zebrafish, *Sox10-Cre* driven RFP signals were not found in taste buds at 15 dpf (n=3), 30 dpf (n=3), and adult stages (n=3) (Figure 6E). However, RFP expression was readily observed in cells within the connective tissue in all tissues examined (Figure 6E). Similar labeling patterns were also found in adult barbels (Figure 6E).

Discussion

Taste bud cells are not derived from neural crest

The neural crest (NC) is a multipotent cell population derived from the lateral ridges of the neural plate in early vertebrate embryos (63). By the fusion of neural folds, NC cells leave the dorsal part of the neural epithelium, migrate extensively and give rise to a wide variety of differentiated cell types, including neurons and glial cells of the peripheral nervous system and connective tissue of the head (12, 16-18, 64). For years, the use of transgenic mouse

lines has facilitated the fate mapping of cranial NC, and findings have led to new speculated NC derivatives, e.g., tooth bud (35) and olfactory (36, 37) epithelial cells. Taste buds have been regarded as solely derived from the surrounding epithelium (26-31). However, recent findings revealed a potential of NC derivation of taste buds in mammals (32-34), thereby suggesting a potential difference in how taste bud cells from in mammals compared to non-mammalian vertebrate.

In the present study we tested the contribution of NC lineage to taste buds in mammals, birds, and teleost fish using *Sox10-iCreER*^{t2}*/tdT* mouse model, GFP^{+}/GFP^{-} chicken chimera model, and *Sox10-Cre/GFP-RFP* zebrafish model. We report that each of these models marks NC lineage specifically or/and extensively. Despite careful examination of multiple individuals in each model, we were unable to find any examples where the NC has contributed to cells in the taste buds. Our data, in combination with those from axolotl (25), provide solid evidence that taste buds, composed largely of glial-like (type I) and neuronal-like (type III) cells, are not derived from NC in mammalian and non-mammalian animals.

Our recent lineage tracing results using *Sox10-Cre* have indicated three candidates of *Sox10*-expressing taste bud progenitors: NC or non-NC derived connective tissue cells in the core of taste papillae, or von Ebner's glands (32). The absence of *Sox10-iCreER*^{T2} (Tmx$^{E7.5}$) labeled cells in taste buds and surrounding epithelium rules out NC as *Sox10*-expressing progenitor for taste buds. This leaves two candidates for future work required to assess the *Sox10*-expressing cell-types under the lingual epithelium (32), including non-NC-derived connective tissue and/or von Ebner's gland (32).

Even though NC does not give rise to taste bud cells, the connective tissue cells in tongue are largely derived from NC (32-34). NC-derived mesenchymal cells interact with the overlying epithelium and play essential roles in taste bud and taste papilla development (65-67). For examples, mesenchymal FGF10 has been reported to control the size of fungiform papillae via modulating epithelial Wnt/β-catenin signals (65); and mesenchymal Follistatin modulates epithelial BMP7 signaling to control size and spacing of fungiform papillae and inhibits gustatory fate of intermolar eminence (66). Future studies using high throughput techniques will be beneficial for identifying novel factors from NC derivatives that are required for taste bud formation and maintenance.

NC lineage tracing: limitations of *Cre* mouse models and ideal using *Sox10-iCreER^{T2}*

Cre/loxP site-specific recombination system is a noninvasive approach that enables long-term lineage tracing. In the past several years, a number of *Cre* mouse lines have been generated for NC lineage tracing (39). For many lines, labeling specificity has been a problem because of ectopic expression of the *Cre* transgene and/or labeling of markers in cells/tissues beyond NC. Additionally, the use of non-inducible *Cre* can lead to labeling of cell lineages from more than one specific cell type. For example, *Wnt1-Cre* mainly labeled the mesencephalic stream of NC (39, 40), which only partially contributes to pharyngeal arch 1 (38), the primordium of the tongue. In addition, ectopic *Wnt1* expression from *Wnt1-Cre* transgene impaired midbrain development (68), and subsequently affected overall development of the mouse. *P0-Cre* mainly the labeled rhombencephalic stream of NC (40), which is a major contributor to pharyngeal arches (38). However, the expression of *P0-Cre* was not NC lineage-restricted, e.g., *P0-Cre* labeled cells were also found in notochord (40),

and ectoderm-derived non-gustatory lingual epithelium at embryonic stages (34, 69). *Dermo1-Cre* has frequently been used to target mesenchymal cell lineages (70-73), however, instead of NC-derived cell labeling only, *Dermo1-Cre* also labeled mesoderm-derived mesenchymal cells, e.g., osteoblasts, chondrocytes (74), perichondrial, and periosteal cells in the trunk and part of the head region (75). *Sox10* is a specific marker for NC cells during early embryonic stages (49, 50). In a previous study using *Sox10-Cre* to trace the lineage of *Sox10*-expressing cells in mouse model, *Sox10* expression was found in cells beyond NC cell lineage, e.g., von Ebner's gland cells under taste papillae (32). Together, careful attention must be paid when using these *Cre* mouse models for tracing NC cell lineages in order to avoid erroneous conclusions about the labeled cell types (34). Indeed, inconsistent observations were obtained in our previous mouse studies using *Wnt1-Cre* (34), *P0-Cre* (33, 34), *Dermo1-Cre* (33), and *Sox10-Cre* (32) driver lines to trace the lineage of NC to taste buds, which raises suspicions about the specificity of those models in labeling the NC lineage.

To test our findings of potential NC origin of taste buds in *Sox10-Cre* as well as other *Cre*-driver lines in previous studies, we introduced an inducible *Cre* model *Sox10-iCreER*^{T2} (41) to specifically target *Sox10*-expressing NC lineage. CreER^{T2} is a fusion protein of Cre recombinase and mutant form of the human estrogen receptor that blocks the nuclear translocation of Cre without exposure to tamoxifen (76). We showed that tamoxifen administration in a given time window when *Sox10* expression was exclusive in migrating NC cells triggered *Cre* recombination in NC cells, labeling them and their derivatives. We found that a single dose of tamoxifen administration at E7.5 was reliable and sufficient for DNA

recombination in NC cells, and that well-known NC derivatives were extensively labeled. Our data suggest that use of the *Sox10-iCreER*^{T2} line in this way is ideal for NC lineage mapping in mice. This model enables us to generate definitive data to answer whether NC gives rise to particular cell types, e.g., taste bud cells.

GFP$^+$ neural fold insertion in chicken embryos is ideal for longitudinally tracking NC cell lineages *in ovo*

Chickens share the common marker Vimentin with humans in labeling taste bud cells (77), which makes it unique for NC lineage mapping in taste buds and facilitates comparison of findings between these two species. The low survival rate of chimeras up to hatch after neural fold transplantation may limit the NC lineage mapping in post-hatch birds. However, taste buds in chickens develop well before hatching, which makes it a good model to use in the present study.

Neural fold transplantation in avian embryos is a well-established, but technically challenging, method to trace cell lineages of the NC (78-81). The development of lines of transgenic chickens in which GFP is ubiquitously expressed facilitates assessment of migrating NC and their contribution to tissues without staining in GFP$^+$/GFP$^-$ chimeras (43). Such a model system allows for longitudinal *in ovo* observations for NC cell migration and lineage tracing. Even though assays involving dye labeling and retroviral infection of NC cells can facilitate the experimental procedures and increase the post-surgery survival rate, neural fold transplantation is more advantageous in providing a highly specific method in labeling NC cells. Moreover, we compared GFP$^+$ neural fold insertion into the tissue lateral to the neural fold of GFP$^-$ host embryo with neural fold replacement, and found that insertion

increased the embryo survival rate and GFP^+ cells from inserted neural fold precede the GFP^- host cells and occupy the target tissue extensively.

Sox10-Cre zebrafish model is useful for labeling cranial NC cell lineages

Zebrafish is an emerging model with advantages of easily accessible and transparent embryos for genetic manipulation and observation of dynamic developmental processes (45, 55-60). Here we used lines of fish harboring transgenes for *Sox10-EGFP* or *Sox10-Cre* to label NC cells. *Sox10*-derived transgenes in zebrafish have been used by a number of investigators to image NC cells and NC lineages throughout the developing zebrafish embryo (44, 46, 82-84). As a consequence, the expression characteristics of the two established transgenic lines used in the current study are well known. Both lines are known to drive expression in migratory NC cells and their derivatives at all axial levels of the embryo and have been used to study the role of NC in the development of a number of tissues, including craniofacial cartilage, pigment cells, and dorsal root ganglion (44, 46, 82-84). Additionally, both lines are known to drive expression in cells that are not derived from NC, such as in the pectoral fin cartilage, otic epithelium, some neurons and oligodendrocytes of the central nervous system, and in some muscle tissues (39, 44, 46, 82). Several of these non-NC derived cells normally express *Sox10* (85). We confirmed that both the *Sox10-EGFP* and *Sox10-Cre* lines are expressed extensively in cranial NC cells and their lineages in developing and adult zebrafish, including cells that could potentially contribute to taste buds. The complete absence of *Sox10-Cre*–labeled cells in all taste bud cells in juvenile and adult fish demonstrates that the taste buds in zebrafish did not receive a contribution from NC.

In the present study, the use of *Sox10-Cre/GFP-RFP* zebrafish allowed us to map NC derivatives in taste buds. Unlike the *Sox10-Cre* mouse line, *Sox10-Cre* labeled cells were not found in zebrafish taste buds. One possible explanation for the differential expression of these transgenes in mice and zebrafish is that there are species-specific differences in *Sox10* expression outside of the NC. Of note, potential distinct ectopic expression of *Cre* cannot be ignored. Careful attention needs to be paid to validating the behavior of transgenic constructs both within a species and especially when comparing results across species.

Acknowledgments

The authors give thanks to Shi-You Chen, Luke Mortensen, Steven Stice, and Franklin West, (Regenerative Bioscience Center, The University of Georgia, Athen, Georgia) for the discussion and feedbacks; to Mary Redmond Hutson (Duke University, Durham, NC) and Richard Schneider (University of California at San Francisco, San Francisco, CA) as consultants for chicken chimera surgery; to Paul Trainor (Stowers Institute for Medical Research), Prasangi Rajapaksha (University of Kentucky, Lexington, KY), Jason Payne and Robert Beckstead (University of Georgia, Athens, GA) for technical assistance of labeling NC cells in chicken model, and The Jackson Laboratory for transgenic mouse lines. This study was supported by the National Institutes of Health, grant number R01DC012308 and R21DC018089 to HXL; R01NS090645 to JDL.

References

1. Farbman AI. Electron microscope study of the developing taste bud in rat fungiform papilla. Developmental biology. 1965;11(1):110-35.

2. Pumplin DW, Yu C, Smith DV. Light and dark cells of rat vallate taste buds are morphologically distinct cell types. Journal of Comparative Neurology. 1997;378(3):389-410.

3. Barlow LA, Klein OD. Developing and regenerating a sense of taste. Current topics in developmental biology. 111: Elsevier; 2015. p. 401-19.

4. Bartel DL, Sullivan SL, Lavoie ÉG, Sévigny J, Finger TE. Nucleoside triphosphate diphosphohydrolase-2 is the ecto-ATPase of type I cells in taste buds. Journal of Comparative Neurology. 2006;497(1):1-12.

5. Miura H, Scott JK, Harada S, Barlow LA. Sonic hedgehog–expressing basal cells are general post - mitotic precursors of functional taste receptor cells. Developmental Dynamics. 2014;243(10):1286-97.

6. Lawton DM, Furness DN, Lindemann B, Hackney CM. Localization of the glutamate–aspartate transporter, GLAST, in rat taste buds. European Journal of Neuroscience. 2000;12(9):3163-71.

7. Huang T, Ma L, Krimm RF. Postnatal reduction of BDNF regulates the developmental remodeling of taste bud innervation. Developmental biology. 2015;405(2):225-36.

8. Roper SD, Chaudhari N. Taste buds: cells, signals and synapses. Nature Reviews Neuroscience. 2017;18(8):485-97.

9. Murray R. The ultrastructure of taste buds. The ultrastructure of sensory organs. 1973:1-81.

10. Murray RG. Cellular relations in mouse circumvallate taste buds. Microscopy research and technique. 1993;26(3):209-24.

11. Murray RG, Murray A, Fujimoto S. Fine structure of gustatory cells in rabbit taste buds. Journal of ultrastructure research. 1969;27(5-6):444-61.

12. Vega-Lopez GA, Cerrizuela S, Aybar MJ. Trunk neural crest cells: formation, migration and

beyond. International Journal of Developmental Biology. 2017;61(1-2):5-15.

13. Morrison SJ, White PM, Zock C, Anderson DJ. Prospective identification, isolation by flow cytometry, and in vivo self-renewal of multipotent mammalian neural crest stem cells. Cell. 1999;96(5):737-49.

14. Douarin NL, Dulac C, Dupin E, Cameron-Curry P. Glial cell lineages in the neural crest. Glia. 1991;4(2):175-84.

15. Sommer L. Specification of Neural Crest-and Placode-Derived Neurons. Patterning and Cell Type Specification in the Developing CNS and PNS: Comprehensive Developmental Neuroscience. 2013;1:385.

16. Weston JA. A radioautographic analysis of the migration and localization of trunk neural crest cells in the chick. Developmental biology. 1963;6(3):279-310.

17. Le Douarin NM, Teillet M-AM. Experimental analysis of the migration and differentiation of neuroblasts of the autonomic nervous system and of neurectodermal mesenchymal derivatives, using a biological cell marking technique. Developmental biology. 1974;41(1):162-84.

18. Schweizer G, Ayer-Le Lièvre C, Le Douarin NM. Restrictions of developmental capacities in the dorsal root ganglia during the course of development. Cell differentiation. 1983;13(3):191-200.

19. Ladher RK, O'Neill P, Begbie J. From shared lineage to distinct functions: the development of the inner ear and epibranchial placodes. Development. 2010;137(11):1777-85.

20. Begbie J, Brunet J-F, Rubenstein J, Graham A. Induction of the epibranchial placodes. Development. 1999;126(5):895-902.

21. Webb JF, Noden DM. Ectodermal placodes contributions to the development of the vertebrate head. American Zoologist. 1993;33(4):434-47.

22. Baker CV, Bronner-Fraser M. Vertebrate cranial placodes I. Embryonic induction. Developmental biology. 2001;232(1):1-61.

23. Schlosser G. Evolutionary origins of vertebrate placodes: insights from developmental studies and from comparisons with other deuterostomes. Journal of Experimental Zoology Part B: Molecular and Developmental Evolution. 2005;304(4):347-99.

24. Streit A. Early development of the cranial sensory nervous system: from a common field to individual placodes. Developmental biology. 2004;276(1):1-15.

25. Barlow LA, Northcutt RG. Embryonic origin of amphibian taste buds. Developmental biology. 1995;169(1):273-85.

26. Hamamichi R, Asano-Miyoshi M, Emori Y. Taste bud contains both short-lived and long-lived cell populations. Neuroscience. 2006;141(4):2129-38.

27. Nguyen HM, Barlow LA. Differential expression of a BMP4 reporter allele in anterior fungiform versus posterior circumvallate taste buds of mice. BMC neuroscience. 2010;11(1):129.

28. Stone LM, Finger TE, Tam P, Tan S-S. Taste receptor cells arise from local epithelium, not neurogenic ectoderm. Proceedings of the National Academy of Sciences. 1995;92(6):1916-20.

29. Okubo T, Clark C, Hogan BL. Cell lineage mapping of taste bud cells and keratinocytes in the mouse tongue and soft palate. Stem cells. 2009;27(2):442-50.

30. Miura H, Barlow LA. Taste bud regeneration and the search for taste progenitor cells. Archives italiennes de biologie. 2010;148(2):107.

31. Hirota M, Ito T, Okudela K, Kawabe R, Hayashi H, Yazawa T, et al. Expression of cyclin-dependent kinase inhibitors in taste buds of mouse and hamster. Tissue and Cell. 2001;33(1):25-32.

32. Yu W, Ishan M, Yao Y, Stice SL, Liu H-X. SOX10-Cre-Labeled Cells Under the Tongue Epithelium Serve as Progenitors for Taste Bud Cells That Are Mainly Type III and Keratin 8-Low. Stem Cells and Development. 2020.

33. Boggs K, Venkatesan N, Mederacke I, Komatsu Y, Stice S, Schwabe RF, et al. Contribution of underlying connective tissue cells to taste buds in mouse tongue and soft palate. PloS one. 2016;11(1).

34. Liu H-X, Komatsu Y, Mishina Y, Mistretta CM. Neural crest contribution to lingual mesenchyme, epithelium and developing taste papillae and taste buds. Developmental biology. 2012;368(2):294-303.

35. Wang S-K, Komatsu Y, Mishina Y. Potential contribution of neural crest cells to dental enamel formation. Biochemical and biophysical research communications. 2011;415(1):114-9.

36. Suzuki J, Yoshizaki K, Kobayashi T, Osumi N. Neural crest-derived horizontal basal cells as tissue stem cells in the adult olfactory epithelium. Neuroscience Research. 2013;75(2):112-20.

37. Katoh H, Shibata S, Fukuda K, Sato M, Satoh E, Nagoshi N, et al. The dual origin of the peripheral olfactory system: placode and neural crest. Molecular brain. 2011;4(1):1-16.

38. O'Rahilly R, Müller F. The development of the neural crest in the human. Journal of anatomy. 2007;211(3):335-51.

39. Debbache J, Parfejevs V, Sommer L. Cre-driver lines used for genetic fate mapping of neural crest cells in the mouse: An overview. genesis. 2018;56(6-7):e23105.

40. Chen G, Ishan M, Yang J, Kishigami S, Fukuda T, Scott G, et al. S pecific and spatial labeling of P0-Cre versus Wnt1-Cre in cranial neural crest in early mouse embryos. genesis. 2017;55(6):e23034.

41. McKenzie IA, Ohayon D, Li H, De Faria JP, Emery B, Tohyama K, et al. Motor skill learning

requires active central myelination. science. 2014;346(6207):318-22.

42. Madisen L, Zwingman TA, Sunkin SM, Oh SW, Zariwala HA, Gu H, et al. A robust and high-throughput Cre reporting and characterization system for the whole mouse brain. Nature neuroscience. 2010;13(1):133.

43. Chapman SC, Lawson A, MacArthur WC, Wiese RJ, Loechel RH, Burgos-Trinidad M, et al. Ubiquitous GFP expression in transgenic chickens using a lentiviral vector. Development. 2005;132(5):935-40.

44. Rodrigues FS, Doughton G, Yang B, Kelsh RN. A novel transgenic line using the Cre–lox system to allow permanent lineage-labeling of the zebrafish neural crest. Genesis. 2012;50(10):750-7.

45. Wada N, Javidan Y, Nelson S, Carney TJ, Kelsh RN, Schilling TF. Hedgehog signaling is required for cranial neural crest morphogenesis and chondrogenesis at the midline in the zebrafish skull. Development. 2005;132(17):3977-88.

46. Carney TJ, Dutton KA, Greenhill E, Delfino-Machín M, Dufourcq P, Blader P, et al. A direct role for Sox10 in specification of neural crest-derived sensory neurons. Development. 2006;133(23):4619-30.

47. Boniface EJ, Lu J, Victoroff T, Zhu M, Chen W. FIEx-based transgenic reporter lines for visualization of Cre and Flp activity in live zebrafish. genesis. 2009;47(7):484-91.

48. Fish JL, Sklar RS, Woronowicz KC, Schneider RA. Multiple developmental mechanisms regulate species-specific jaw size. Development. 2014;141(3):674-84.

49. Southard-Smith EM, Kos L, Pavan WJ. Sox10 mutation disrupts neural crest development in Dom Hirschsprung mouse model. Nature genetics. 1998;18(1):60.

50. Kuhlbrodt K, Herbarth B, Sock E, Hermans-Borgmeyer I, Wegner M. Sox10, a novel transcriptional modulator in glial cells. Journal of Neuroscience. 1998;18(1):237-50.

51. Nichols DH. Ultrastructure of neural crest formation in the midbrain/rostral hindbrain and preotic hindbrain regions of the mouse embryo. American journal of anatomy. 1987;179(2):143-54.

52. Theveneau E, Mayor R. Neural crest delamination and migration: from epithelium-to-mesenchyme transition to collective cell migration. Developmental biology. 2012;366(1):34-54.

53. Kaufman MH. Atlas of mouse development: Academic press; 1992.

54. Giovannone D, Ortega B, Reyes M, El-Ghali N, Rabadi M, Sao S, et al. Chicken trunk neural crest migration visualized with HNK1. Acta histochemica. 2015;117(3):255-66.

55. Raible DW, Wood A, Hodsdon W, Henion PD, Weston JA, Eisen JS. Segregation and early dispersal of neural crest cells in the embryonic zebrafish. Developmental dynamics. 1992;195(1):29-42.

56. Schilling TF, Kimmel CB. Segment and cell type lineage restrictions during pharyngeal arch development in the zebrafish embryo. Development. 1994;120(3):483-94.

57. Kague E, Gallagher M, Burke S, Parsons M, Franz-Odendaal T, Fisher S. Skeletogenic fate of zebrafish cranial and trunk neural crest. PloS one. 2012;7(11).

58. Raible DW, Eisen JS. Restriction of neural crest cell fate in the trunk of the embryonic zebrafish. Development. 1994;120(3):495-503.

59. Lee RTH, Knapik EW, Thiery JP, Carney TJ. An exclusively mesodermal origin of fin mesenchyme demonstrates that zebrafish trunk neural crest does not generate ectomesenchyme. Development. 2013;140(14):2923-32.

60. Lee RTH, Thiery JP, Carney TJ. Dermal fin rays and scales derive from mesoderm, not neural crest. Current Biology. 2013;23(9):R336-R7.

61. Landacre F. The fate of the neural crest in the head of the urodeles. Journal of Comparative Neurology. 1921;33(1):1-43.

62. Mongera A, Singh AP, Levesque MP, Chen Y-Y, Konstantinidis P, Nüsslein-Volhard C. Genetic lineage labeling in zebrafish uncovers novel neural crest contributions to the head, including gill pillar cells. Development. 2013;140(4):916-25.

63. Huang X, Saint-Jeannet J-P. Induction of the neural crest and the opportunities of life on the edge. Developmental biology. 2004;275(1):1-11.

64. Johnston M. Isotretinoin embryopathy in a mouse model: Cranial neural crest involvement. Teratology. 1985;31:26A.

65. Prochazkova M, Häkkinen TJ, Prochazka J, Spoutil F, Jheon AH, Ahn Y, et al. FGF signaling refines Wnt gradients to regulate the patterning of taste papillae. Development. 2017;144(12):2212-21.

66. Beites CL, Hollenbeck PL, Kim J, Lovell-Badge R, Lander AD, Calof AL. Follistatin modulates a BMP autoregulatory loop to control the size and patterning of sensory domains in the developing tongue. Development. 2009;136(13):2187-97.

67. Castillo-Azofeifa D, Losacco JT, Salcedo E, Golden EJ, Finger TE, Barlow LA. Sonic hedgehog from both nerves and epithelium is a key trophic factor for taste bud maintenance. Development. 2017;144(17):3054-65.

68. Lewis AE, Vasudevan HN, O'Neill AK, Soriano P, Bush JO. The widely used Wnt1-Cre transgene causes developmental phenotypes by ectopic activation of Wnt signaling. Developmental biology. 2013;379(2):229-34.

69. Kawakami M, Umeda M, Nakagata N, Takeo T, Yamamura K-i. Novel migrating mouse neural crest cell assay system utilizing P0-Cre/EGFP fluorescent time-lapse imaging. BMC Developmental

Biology. 2011;11(1):1-17.

70. Cornett B, Snowball J, Varisco BM, Lang R, Whitsett J, Sinner D. Wntless is required for peripheral lung differentiation and pulmonary vascular development. Developmental biology. 2013;379(1):38-52.

71. Geske MJ, Zhang X, Patel KK, Ornitz DM, Stappenbeck TS. Fgf9 signaling regulates small intestinal elongation and mesenchymal development. Development. 2008;135(17):2959-68.

72. Lin C, Yin Y, Long F, Ma L. Tissue-specific requirements of β-catenin in external genitalia development. Development. 2008;135(16):2815-25.

73. Yin Y, White AC, Huh S-H, Hilton MJ, Kanazawa H, Long F, et al. An FGF–WNT gene regulatory network controls lung mesenchyme development. Developmental biology. 2008;319(2):426-36.

74. Yu K, Xu J, Liu Z, Sosic D, Shao J, Olson EN, et al. Conditional inactivation of FGF receptor 2 reveals an essential role for FGF signaling in the regulation of osteoblast function and bone growth. Development. 2003;130(13):3063-74.

75. Li L, Cserjesi P, Olson EN. Dermo-1: a novel twist-related bHLH protein expressed in the developing dermis. Developmental biology. 1995;172(1):280-92.

76. Hirrlinger PG, Scheller A, Braun C, Hirrlinger J, Kirchhoff F. Temporal control of gene recombination in astrocytes by transgenic expression of the tamoxifen-inducible DNA recombinase variant CreERT2. Glia. 2006;54(1):11-20.

77. Witt M, Reutter K, Ganchrow D, Ganchrow JR. Fingerprinting taste buds: intermediate filaments and their implication for taste bud formation. Philosophical Transactions of the Royal Society of London Series B: Biological Sciences. 2000;355(1401):1233-7.

78. Le Douarin N. A biological cell labeling technique and its use in experimental embryology.

Developmental biology. 1973;30(1):217-22.

79. Douarin L. Developmental Relationships between the Neural Crest and the Polypeptide-Hormone-Secreting Cells. The Neural Crest Cambridge. 1982:91-107.

80. Le Lièvre CS, Le Douarin N. Mesenchymal derivatives of the neural crest: analysis of chimaeric quail and chick embryos. Development. 1975;34(1):125-54.

81. Noden DM. The role of the neural crest in patterning of avian cranial skeletal, connective, and muscle tissues. Developmental biology. 1983;96(1):144-65.

82. Dutton JR, Antonellis A, Carney TJ, Rodrigues FS, Pavan WJ, Ward A, et al. An evolutionarily conserved intronic region controls the spatiotemporal expression of the transcription factor Sox10. BMC developmental biology. 2008;8(1):105.

83. Kwak J, Park OK, Jung YJ, Hwang BJ, Kwon S-H, Kee Y. Live image profiling of neural crest lineages in zebrafish transgenic lines. Molecules and cells. 2013;35(3):255-60.

84. Kague E, Gallagher M, Burke S, Parsons M, Franz-Odendaal T, Fisher S. Skeletogenic fate of zebrafish cranial and trunk neural crest. PloS one. 2012;7(11):e47394.

85. Dutton KA, Pauliny A, Lopes SS, Elworthy S, Carney TJ, Rauch J, et al. Zebrafish colourless encodes sox10 and specifies non-ectomesenchymal neural crest fates. Development. 2001;128(21):4113-25.

Figure 1. Sufficiency of a single dose of tamoxifen (Tmx) in activating the nuclear translocation of Cre recombinase that triggered DNA recombination to drive tdT expression in NC and NC-derived tissues. **A-B:** Low (A) and high (B) -power images of transverse sections of the cranial region of a vehicle (Veh)-treated *Sox10-iCreER^{T2}* mouse embryo at E8.5 (12-somite). Immunosignals of Cre (green) in the cytoplasm (arrowheads in B) and Sox10 (magenta) in the nuclei were visualized. White dashed lines in A outline the foregut diverticulum with non-specific staining (40). TN: trigeminal NC tissue; BA1: branchial arch 1; OE: optic eminence. **C:** High-magnification images of the BA1 region in a transverse section of an E8.5 (9-somite) *Sox10-iCreER^{T2}* mouse embryo with tamoxifen activation of *Cre* (Tmx$^{E7.5}$). Arrows point to the Cre immunosignals (green) within nuclei. **D:** Images of whole mount (D_1) and sagittal section (D_2) of the tongue from a E12.5 *Sox10-iCreER^{T2}/tdT* mouse embryo with tamoxifen activation of *Cre* (Tmx$^{E7.5}$). Tongue epithelium was immunoreacted with antibody against E-cadherin (green) in D_2. **E:** Bright field (E_1) and tdT fluorescent (E_2) images of mouse dorsal root ganglia (arrows) of a *Sox10-iCreER^{T2}/tdT* mouse at 8 wk with tamoxifen activation of *Cre* (Tmx$^{E7.5}$). Arrows point to the dorsal root ganglia. Scale bars: 50 μm in A and D (single-plane laser scanning confocal); 10 μm in B and C (single-plane laser scanning confocal); 1 mm in E (stereomicroscopy).

Figure 2. Single-plane laser scanning confocal photomicrographs to demonstrate the distributions of *Sox10-iCreER^{T2}/tdT*-labeled cells in the tongue and soft palate in postnatal mice (Tmx$^{E7.5}$) at different stages. **A-B:** Images of a fungiform papilla on a sagittal section (A_1, B_1) and circumvallate on a coronal section (A_2, B_2) of tongue at 2 wk (A) and 4 wk (B). **C:** Images of soft palate (C_1), fungiform papilla (C_2), foliate papilla on a sagittal section (C_3), and circumvallate papilla on a coronal section (C_4) of tongue tissue at 8 wk. Taste buds were marked by the immunosignals of Keratin 8 (Krt8, green). White dashed lines demarcate lingual epithelium from the underlying connective tissue. Scale bars: 50 μm for all images.

Figure 3. Migration of GFP^+ NC cells ventrally in GFP^- host chicken after the insertion of the GFP^+ neural fold. **A**: A schematic graph illustrating the insertion of GFP^+ neural fold to GFP^- host chicken. **B**: Photomicrographs of a GFP^+/GFP^- chicken chimera at 1 DPS. Top: fluorescent image to show GFP signals; Bottom: merged fluorescent and bright-field images. **C**: Single-plane laser scanning confocal images of a section (C_1) from the position indicated by white line in B and higher power images (C_2) from the area indicated by dashed square shown in C_1. Sections were immunoreacted for NC cell marker HNK1 (magenta). Scale bars: 500 μm in B; 80 μm in C_1 and 20 μm in C_2.

Figure 4. Distribution of GFP^+ neural fold-derived cells in the craniofacial regions ispilateral to the surgery side. **A**: Photomicrographs of a chimeric embryo at 2 DPS, side view of heads and dorsal view of the lower beak (LB) at 14 and 19 DPS, and upper beak (UP) at 19 DPS. Top panel: fluorescent images to show the GFP signals; Bottom panel: merged fluorescent and bright-field images. **B**: Single-plane laser scanning confocal images of sagittal sections of pharyngeal arch of chimeric embryo at 2 DPS and base of oral cavities of chimeric embryos at 14 and 19 DPS. Sections were immunoreacted for the epithelial cell marker EpCAM (magenta). White dashed lines demarcate the epithelium from the underlying mesenchyme. Scale bars: 2 mm in A; 20 μm in B.

Figure 5. Distribution of GFP^+ labeled cells in the tissue of oral cavity of chimeric embryos at 19 DPS. **A**: Representative images of a sagittal section of the base of oral cavity. **B**: Images of a sagittal section of the palate. Sections were immunoreacted for taste bud cell marker α-Gustducin (magenta). White dashed lines encircle taste buds. Autofluorescence in α-Gustducin immunoreacted sections were identified and are marked by asterisks (*). Scales bars: 20 μm for all images (single-plane laser scanning confocal images).

Figure 6. Mapping NC cell lineages in zebrafish. **A-C**: *Sox10-EGFP* expression was in NC but not in taste buds. **A**: Merges EGFP and bright-field images of lateral views of *Sox10-EGFP* fish embryos at 7, 10, and 12-somite stages. Arrowheads point to heads and arrows point to truck regions. **B**: Photomicrographs of transverse sections of cranial regions of a 12-somite *Sox10-EGFP* fish embryo. Migrating NC cells were immunostained for Sox10 (magenta). **C**: Photomicrographs of a sagittal section of a taste bud in lower jaw of a 5.5 dpf fish embryo. **D-E**: *Sox10-Cre/GFP-RFP* labeled known NC-derived tissues but not taste buds. **D**: Whole mount images of gills (arrows) of *Sox10-Cre/GFP-RFP* adult zebrafish. **E**: Photomicrographs of sagittal sections of lower jaws at 15 dpf, 30 dpf, and adult and adult barbel of *Sox10-Cre/GFP-RFP* zebrafish. GFP and RFP signals were amplified by applying antibodies against GFP (green) and RFP (magenta). Calretinin (gray) indicates presence of taste buds. Scale bars: 200 μm in A and D; 50 μm in B; 20 μm in C and E (single-plane laser scanning confocal).

Table 1

Table 1. Primary antibodies that were used.

Antibodies	Dilution	Source
mouse anti-Calretinin clone 6B3	1:5000 (section) 1:1000 (whole mount)	Cat No. 010399, Swant, Switzerland
goat anti-Cre	1:500	Cat No.sc-83398, Santa Cruz Biotechnology, INC. Dallas, TX
rabbit anti-dsRed	1:500	Cat No. ab62341, Abcam, UK
goat anti-E-cadherin	1:500	Cat No. AF748, Fisher Scientific, Waltham, MA
chicken anti-GFP	1:500 (section) 1:250 (whole mount)	Cat No. GFP-1010, Aves Labs, Tigard, OR
rat anti-Keratin 8 (Krt8)	1:1000	Cat No. TROMA-1, Developmental Studies Hybridoma Bank, Iowa city, IA
goat anti-SOX10	1:500	Cat No. sc-365692, Santa Cruz Biotechnology, Dallas, TX
mouse anti- HNK1(1C10)	1:10	Cat No. AB_10570406, Developmental Studies Hybrydoma Bank, Iwoa city, IA
rabbit anti-Epithelial Cell Adhesion Molecule markers (EpCAM)	1:200	Cat No. MBS2027145, Mybioresource Inc, San Diego, CA
rabbit anti-α-Gustducin	1:500	Generated by Dr. Shoji Tabata's lab
mouse anti-Vimentin (Vim3B4)	1:250	Cat No. ab28028, Abcam, UK

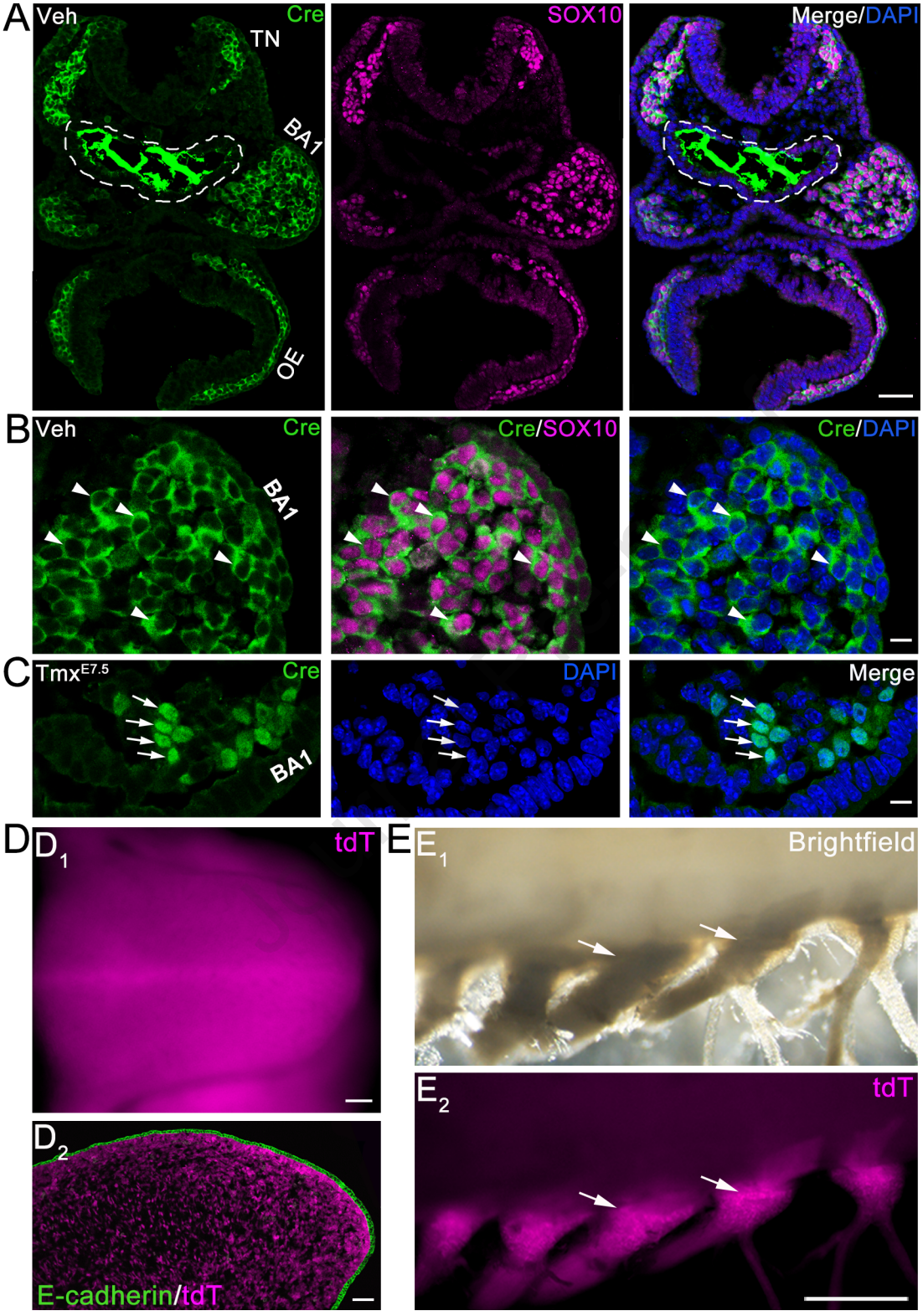
A
Veh
Cre
TN
BA1
OE
SOX10
Merge/DAPI
B
Veh
Cre
BA1
Cre/SOX10
Cre/DAPI
C
Tmx$^{E7.5}$
Cre
BA1
DAPI
Merge
D
D$_1$
tdT
D$_2$
E-cadherin/tdT
E
E$_1$
Brightfield
E$_2$
tdT

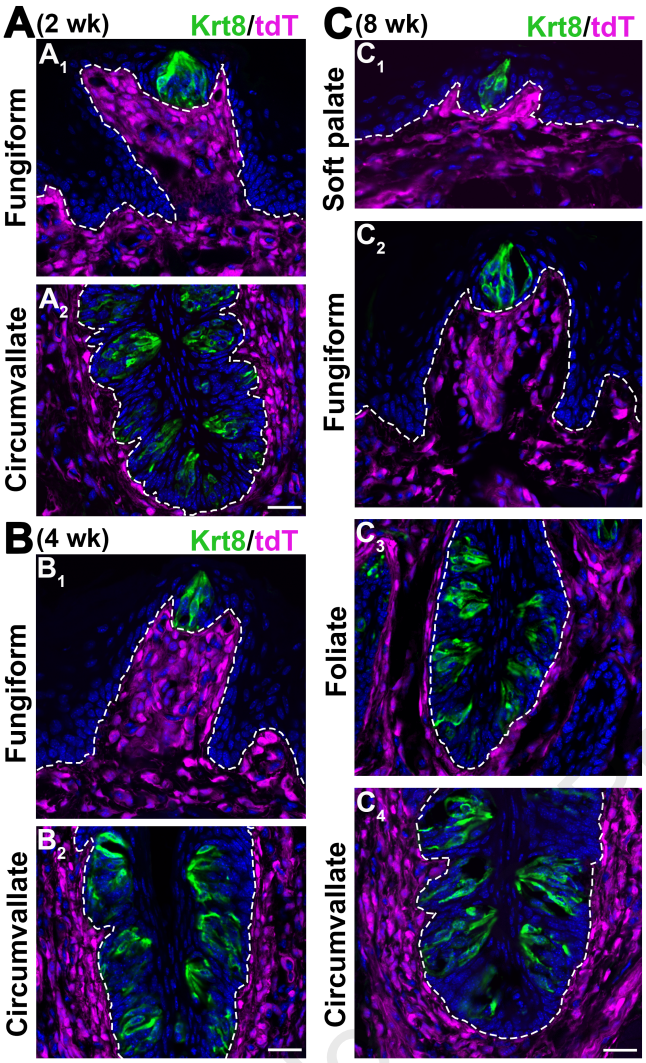

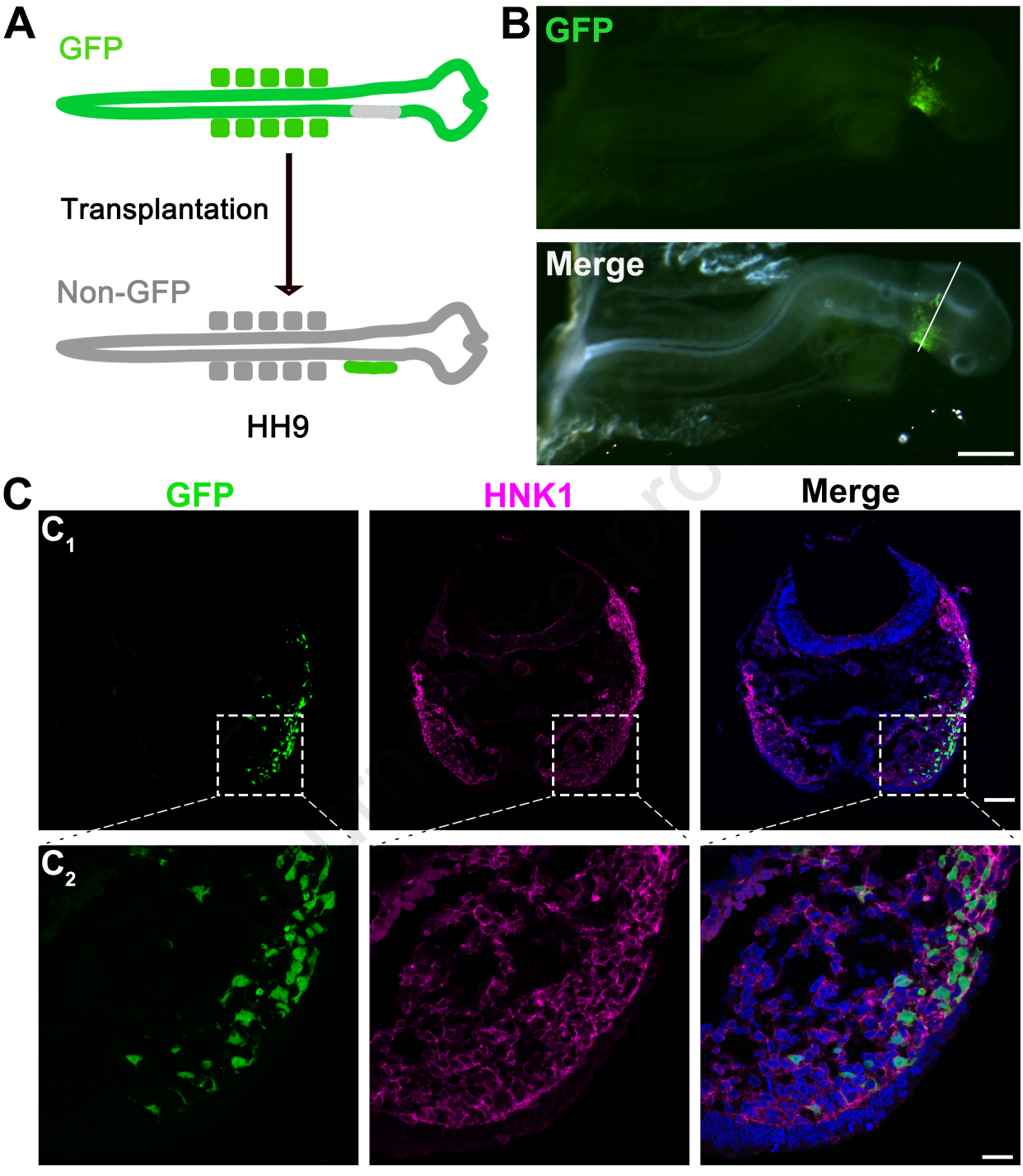
A
GFP
Transplantation
Non-GFP
HH9
B
GFP
Merge
C
GFP
HNK1
Merge
C1
C2

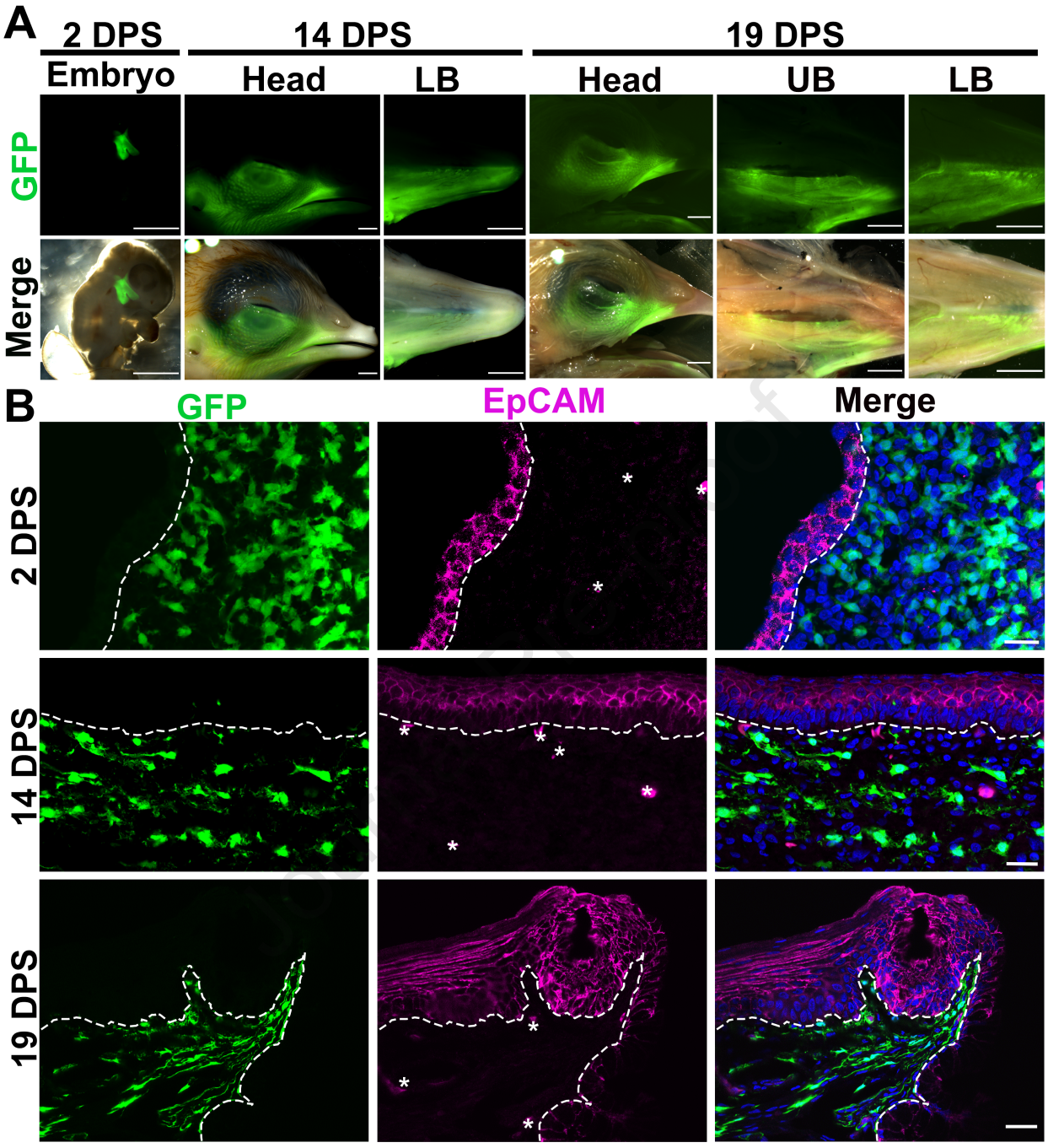
A
2 DPS
14 DPS
19 DPS
Embryo
Head
LB
Head
UB
LB
GFP
Merge
B
GFP
EpCAM
Merge
2 DPS
14 DPS
19 DPS

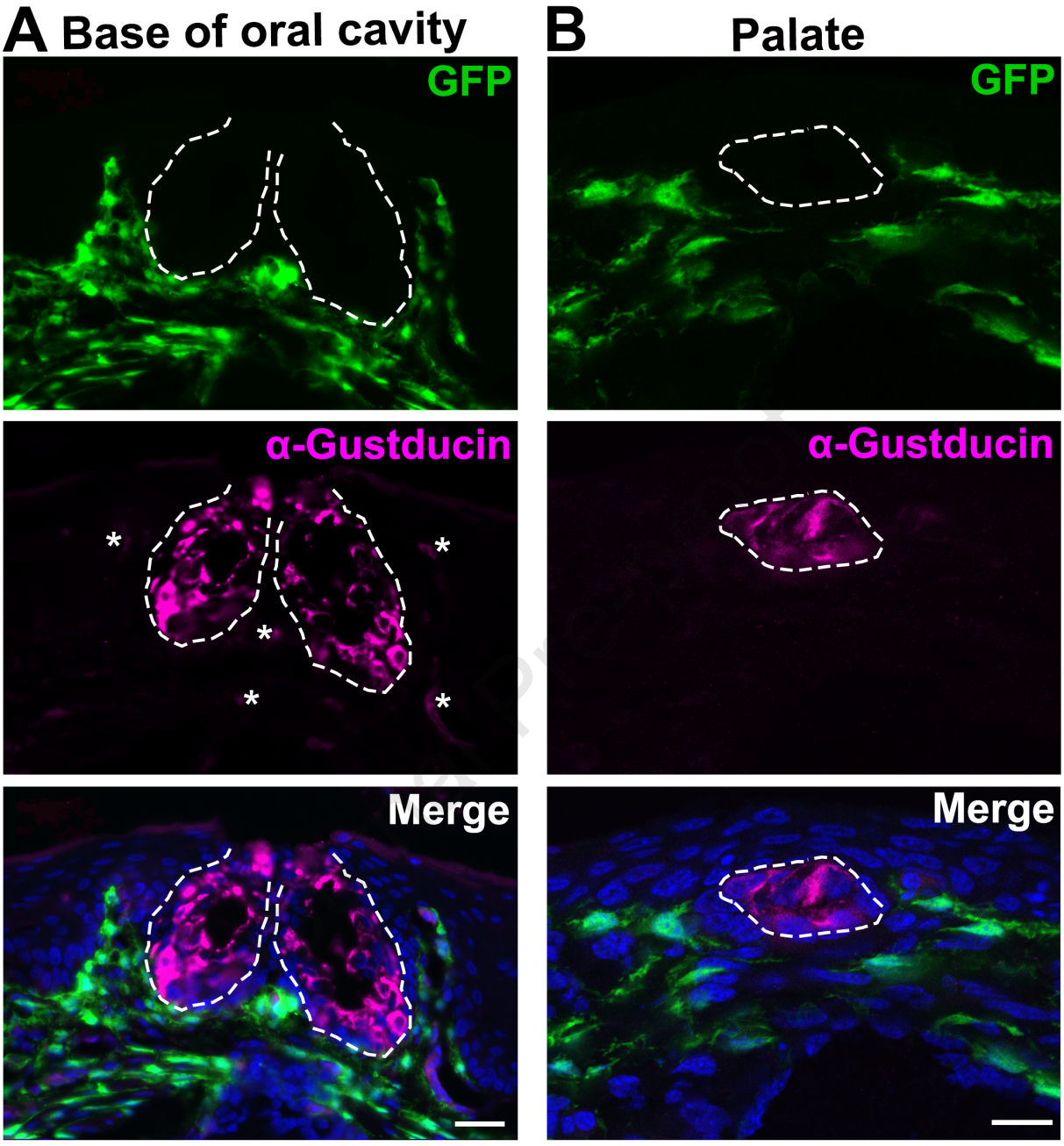
A Base of oral cavity
B Palate
GFP
GFP
α-Gustducin
α-Gustducin
Merge
Merge

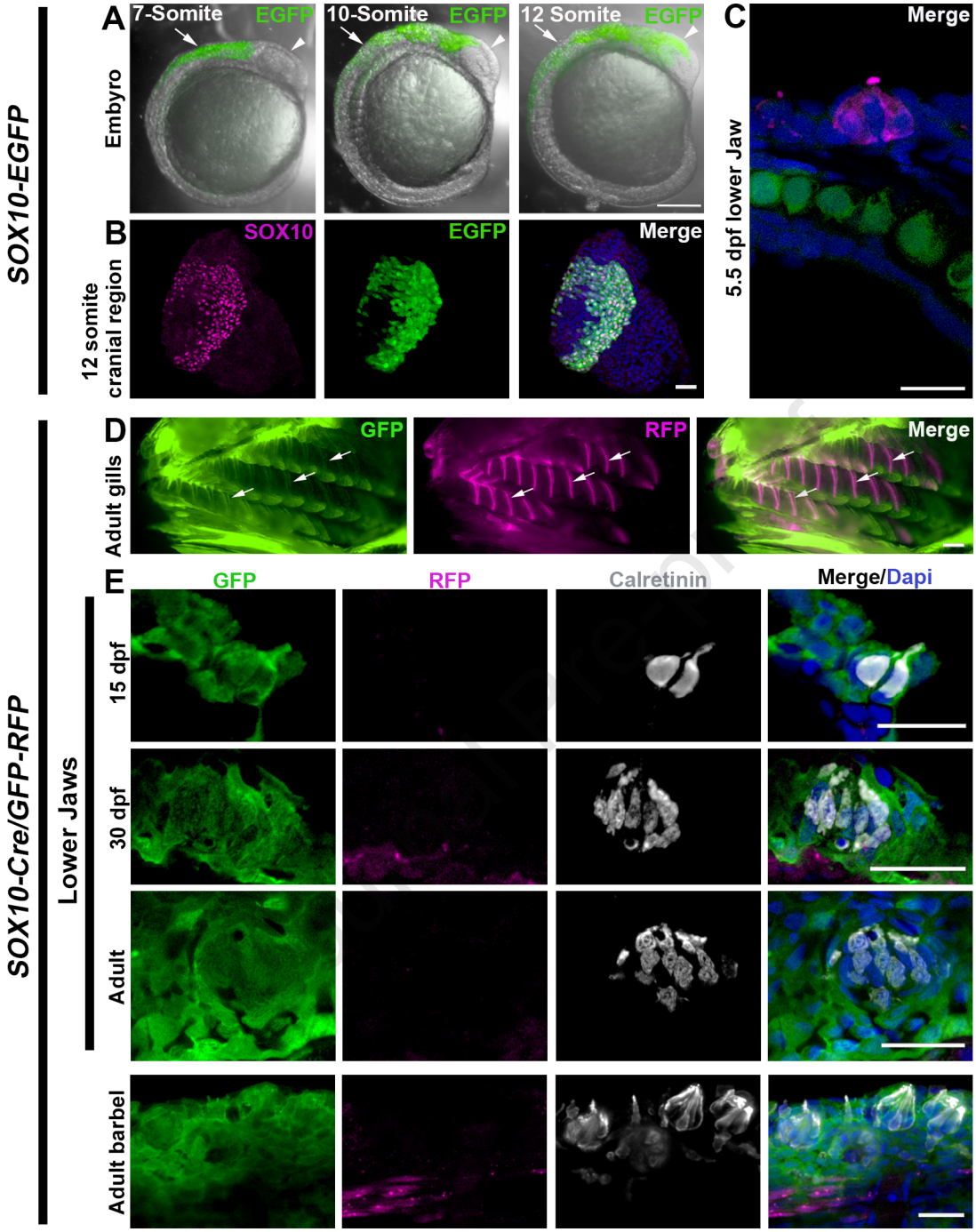
SOX10-EGFP
A
7-Somite
EGFP
10-Somite
EGFP
12 Somite
EGFP
Embyro
B
SOX10
EGFP
Merge
12 somite cranial region
C
Merge
5.5 dpf lower Jaw
SOX10-Cre/GFP-RFP
D
GFP
RFP
Merge
Adult gills
E
GFP
RFP
Calretinin
Merge/Dapi
Lower Jaws
15 dpf
30 dpf
Adult
Adult barbel

Highlights:

(1) Neural crest-derived cells are not seen in taste buds in mouse, chicken, and zebrafish.

(2) *Sox10-iCreER*^{T2} is ideal for neural crest lineage mapping in mouse.

(3) GFP^{+}/GFP^{-} chicken chimera is valuable for longitudinally tracking neural crest cells.